optica

Guiding and confining of light in a two-dimensional synthetic space using electric fields: supplementary material

HAMIDREZA CHALABI[1,2,*], SABYASACHI BARIK[1,2,3], SUNIL MITTAL[1,2], THOMAS E. MURPHY[1,3], MOHAMMAD HAFEZI[1,2,3], AND EDO WAKS[1,2,3,**]

[1]Department of Electrical and Computer Engineering and Institute for Research in Electronics and Applied Physics, University of Maryland, College Park, Maryland, 20742, USA

[2]Joint Quantum Institute, University of Maryland, College Park, Maryland, 20742, USA

[3]Department of Physics, University of Maryland, College Park, Maryland, 20742, USA

[*]hchalabi@umd.edu

[**]edowaks@umd.edu

Published 12 May 2020

This document provides supplementary information to "Guiding and confining of light in a two-dimensional synthetic space using electric fields," https://doi.org/10.1364/OPTICA.386347. We explain the experimental details of this study in the first section of this supplemental material. In the second section, we review the theoretical analysis of one-dimensional quantum walks and explain the possibility of observing Bloch oscillations using time-dependent gauge fields in such quantum walks. In the next section, we provide the corresponding theoretical analysis for the case of two-dimensional quantum walks.

1. EXPERIMENTAL DETAILS:

Figure S1 shows the schematic of the experimental setup, which is composed of similar elements as used in our previous work [1]. However, the phase modulation patterns used in this study are different from those used earlier. We used a laser diode made by Bookham technology (LC25W5172BA-J34) operating at the C-band of the telecom wavelength (1550 nm) for pulse generation. By modulating this laser, pulses with a power of $10\,mW$ and pulse duration of $2\,ns$ were generated, which were sent into the setup with a repetition rate of $10\,\mu s$. These pulses initiate the quantum walk in our synthetic two-dimensional space. The initial pulse after passing through the first 50/50 beam splitter continues its path through either the 1 m or 2 m fiber length. This leads to different delays that can be conceptually regarded as "choosing" the left or right direction in the x movement by the quantum walker. When reaching the next beam splitter, the pulse chooses either the 130 m or 118 m fiber spool. This determines whether the pulse has gone in the up or down direction in the y movement. The x and y coordinate of the pulses are encoded based on the delay in reaching the detectors. We used 90/10 beam splitters to out-couple 10% of the light for detection purposes. In addition, two phase modulators made by Cybel, LLC (MPZ-LN-10-P-P-FA-FA) were used to apply opposite phases to the right and left moving pulses (i.e., $\pm x$ direction).

We used semiconductor optical amplifiers made by Thorlabs (SOA1117S) to compensate for the loss in the setup by amplifying the pulses without ruining their phase coherence. These amplifiers are only turned on for a fraction of a repetition period at each cycle to avoid over amplifying the background noises. Moreover, in order to filter out background noises, we used narrow band-pass filters ($< 0.3nm$) directly after the semiconductor optical amplifiers. However, the ratio of the optical pulse power at different positions of the synthetic space relative to the noise degrades with increasing time steps due to the diffusion and the added noise. We therefore limited our measurement of the quantum walk distribution to 10 steps because of the observed degradation of the signal-to-noise ratio and the finite ratio of the time delays corresponding to the x and y movements. The distribution of the quantum walk at every time step was determined by measuring the power of the pulses present in each step. We also used polarization controllers in our setup in order to compensate for the polarization changes along the optical fibers.

We measured the quantum walk distribution at different time steps under the application of the proposed time-varying gauge fields with different phases ($\phi = 0\,[deg]$, $\phi = 90\,[deg]$, $\phi = 60\,[deg]$, $\phi = 45\,[deg]$, and$\phi = 36\,[deg]$).

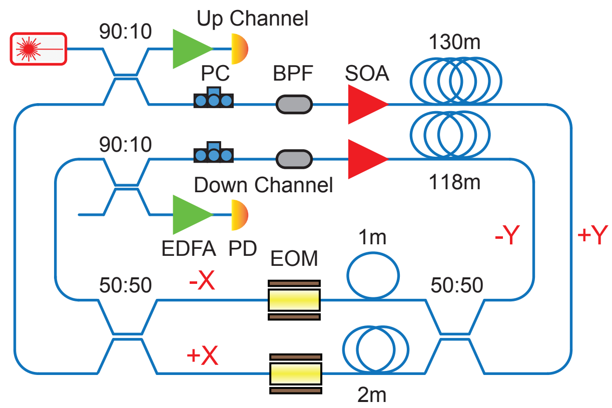

Fig. S1. Schematic of the experimental setup for the two-dimensional quantum random walk. PD: photodetector, BPF: band-pass filter, SOA: semiconductor optical amplifier, EDFA: Erbium-doped fiber amplifier, EOM: Electro-optic modulator and PC: polarization controller.

Using the measured probability distributions, we calculated the quadratic means and norm ones of the x and y of the quantum walk distribution. We plotted the variation of these quantities by the time step in the main text. These quantities reach their local minima after around $2\pi/\phi$ time steps depending on the value of ϕ used. This behavior is due to the state revival and the trapping of the quantum walk distribution close to the origin after around $2\pi/\phi$ time steps.

Based on the measured results, we can also calculate the quantum walk distribution probability at the origin for different applied phases. Using these probabilities, we plotted the revival probability in the main text as a function of the required steps to reach the revival. Indeed, smaller phases lead to higher probability of the revival, as has been discussed in the main text.

We note that the error in our measurement of the intensity of the pulses at different time delays (corresponding to different positions in the synthetic space) is around 3% ($\Delta P_{x,y}/P_{x,y} = 3\%$). This error will propagate to the error in the calculated quadratic means, norm ones, and revival probabilities, as explained in the following.

By defining $P_1 = \sum_{x,y} x^2 P_{x,y}$ and $P_2 = \sum_{x,y} P_{x,y}$, in which $P_{x,y}$ is the power detected at coordinates x and y in the synthetic space, the quadratic mean of x is calculated based on:

$$x_{rms} = \sqrt{< x^2 >} = \sqrt{\frac{\sum_{x,y} x^2 P_{x,y}}{\sum_{x,y} P_{x,y}}} = \sqrt{\frac{P_1}{P_2}}. \tag{S1}$$

By assuming that $\Delta P_{x,y}/P_{x,y} = D = 3\%$, since $x^2 > 0$ and $P_{x,y} > 0$, then:

$$\frac{\Delta P_1}{P_1} = \frac{\sqrt{\sum_{x,y} x^4 \left(\Delta P_{x,y}\right)^2}}{\sum_{x,y} x^2 P_{x,y}} = \frac{D\sqrt{\sum_{x,y} x^4 P_{x,y}^2}}{\sum x^2 P_{x,y}} \leq D \tag{S2}$$

$$\frac{\Delta P_2}{P_2} = \frac{\sqrt{\sum_{x,y} \left(\Delta P_{x,y}\right)^2}}{\sum_{x,y} P_{x,y}} = \frac{D\sqrt{\sum_{x,y} P_{x,y}^2}}{\sum_{x,y} P_{x,y}} \leq D \tag{S3}$$

Therefore:

$$\frac{\Delta < x^2 >}{< x^2 >} = \sqrt{\left(\frac{\Delta P_1}{P_1}\right)^2 + \left(\frac{\Delta P_2}{P_2}\right)^2} \leq \sqrt{2}D \tag{S4}$$

Consequently:

$$\frac{\Delta x_{rms}}{x_{rms}} = \frac{1}{2}\frac{\Delta < x^2 >}{< x^2 >} \leq \frac{1}{\sqrt{2}}D \tag{S5}$$

Similarly, by defining $P_3 = \sum_{x,y} |x| P_{x,y}$, the norm one of x is calculated based on:

$$< |x| > = \frac{P_3}{P_2} \tag{S6}$$

Since $|x| > 0$ and $P_{x,y} > 0$, then:

$$\frac{\Delta P_3}{P_3} = \frac{\sqrt{\sum_{x,y} x^2 \left(\Delta P_{x,y}\right)^2}}{\sum_{x,y} |x| P_{x,y}} = \frac{D\sqrt{\sum_{x,y} x^2 P_{x,y}^2}}{\sum |x| P_{x,y}} \leq D \tag{S7}$$

Consequently:

$$\frac{\Delta < |x| >}{< |x| >} = \sqrt{\left(\frac{\Delta P_3}{P_3}\right)^2 + \left(\frac{\Delta P_2}{P_2}\right)^2} \leq \sqrt{2}D \tag{S8}$$

A similar analysis holds for the y direction.
The probability of revival is also calculated based on:

$$P_U(0,0) = \frac{P_{0,0}}{\sum_{x,y} P_{x,y}} \tag{S9}$$

Consequently:

$$\frac{\Delta P_U(0,0)}{P_U(0,0)} = \sqrt{\left(\frac{\Delta P_{0,0}}{P_{0,0}}\right)^2 + \left(\frac{\Delta P_2}{P_2}\right)^2} \leq \sqrt{2}D \tag{S10}$$

Therefore, the error bars in the quadratic means and norm ones as well as the probabilities of revival are less than around 4% and are smaller than the size of the plotted data points.

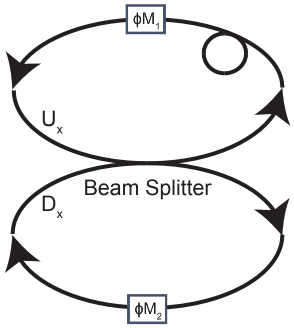

Fig. S2. Simplified version of the schematic of a one-dimensional quantum random walk setup

2. THEORETICAL ANALYSIS FOR ONE-DIMENSIONAL QUANTUM RANDOM WALKS:

In this section, we consider the evolution of pulses (representing the quantum walkers) in one-dimensional quantum random walks. For the theoretical analysis of the quantum walk, we can assume that all the losses in the setup are fully compensated by the amplifiers. Therefore, we can consider an ideal setup as shown in Fig. S2.

Two pulses just before the first beam splitter, $\begin{bmatrix} U_x^{(n)} \\ D_x^{(n)} \end{bmatrix}$, will produce the output pulses as (movement in the x direction):

$$\begin{bmatrix} U_{x+1}^{(n+1)} \\ D_{x-1}^{(n+1)} \end{bmatrix} = \frac{1}{\sqrt{2}} \begin{bmatrix} e^{-i\phi_{n,x}} & 0 \\ 0 & e^{i\phi_{n,x}} \end{bmatrix} \times \begin{bmatrix} 1 & -1 \\ 1 & 1 \end{bmatrix} \begin{bmatrix} U_x^{(n)} \\ D_x^{(n)} \end{bmatrix}. \quad \text{(S11)}$$

Therefore, $\begin{bmatrix} U_x^{(n)} \\ D_x^{(n)} \end{bmatrix}$ will produce the following pulses after traversing the beam splitter:

$$U_{x+1}^{(n+1)} = \frac{e^{-i\phi_{n,x}}}{\sqrt{2}} \left(U_x^{(n)} - D_x^{(n)} \right) \quad \text{(S12)}$$

$$D_{x-1}^{(n+1)} = \frac{e^{i\phi_{n,x}}}{\sqrt{2}} \left(U_x^{(n)} + D_x^{(n)} \right) \quad \text{(S13)}$$

Alternatively, based on the above results $\begin{bmatrix} U_x^{(n+1)} \\ D_x^{(n+1)} \end{bmatrix}$ can be produced from other pulses as:

$$U_x^{(n+1)} = \frac{e^{-i\phi_{n,x-1}}}{\sqrt{2}} \left(U_{x-1}^{(n)} - D_{x-1}^{(n)} \right) \quad \text{(S14)}$$

$$D_x^{(n+1)} = \frac{e^{i\phi_{n,x+1}}}{\sqrt{2}} \left(U_{x+1}^{(n)} + D_{x+1}^{(n)} \right) \quad \text{(S15)}$$

By defining $S_x^{(n)} = U_x^{(n)} + D_x^{(n)}$ and $P_x^{(n)} = U_x^{(n)} - D_x^{(n)}$, the obtained equations can be written as:

$$S_x^{(n+1)} = \frac{e^{i\phi_{n,x+1}}}{\sqrt{2}} S_{x+1}^{(n)} + \frac{e^{-i\phi_{n,x-1}}}{\sqrt{2}} P_{x-1}^{(n)} \quad \text{(S16)}$$

$$P_x^{(n+1)} = -\frac{e^{i\phi_{n,x+1}}}{\sqrt{2}} S_{x+1}^{(n)} + \frac{e^{-i\phi_{n,x-1}}}{\sqrt{2}} P_{x-1}^{(n)} \quad \text{(S17)}$$

$$\begin{bmatrix} S_x^{(n+1)} \\ P_x^{(n+1)} \end{bmatrix} = \frac{1}{\sqrt{2}} \begin{bmatrix} e^{i\phi_{n,x+1}} & e^{-i\phi_{n,x-1}} \\ -e^{i\phi_{n,x+1}} & e^{-i\phi_{n,x-1}} \end{bmatrix} \begin{bmatrix} S_{x+1}^{(n)} \\ P_{x-1}^{(n)} \end{bmatrix} \quad \text{(S18)}$$

By defining $s_{k_x}^{(n)}$ and $p_{k_x}^{(n)}$ as Fourier transforms of $S_x^{(n)}$ and $P_x^{(n)}$, we have:

$$\begin{bmatrix} S_x^{(n)} \\ P_x^{(n)} \end{bmatrix} = \frac{1}{2\pi} \begin{bmatrix} \int_{k_x} s_{k_x}^{(n)} e^{ik_x x} dk_x \\ \int_{k_x} p_{k_x}^{(n)} e^{ik_x x} dk_x \end{bmatrix} \quad \text{(S19)}$$

Therefore:

$$\begin{bmatrix} \int_{k_x} s_{k_x}^{(n+1)} e^{ik_x x} dk_x \\ \int_{k_x} p_{k_x}^{(n+1)} e^{ik_x x} dk_x \end{bmatrix} = \frac{1}{\sqrt{2}} \begin{bmatrix} e^{i\phi_{n,x+1}} & e^{-i\phi_{n,x-1}} \\ -e^{i\phi_{n,x+1}} & e^{-i\phi_{n,x-1}} \end{bmatrix} \times \begin{bmatrix} \int_{k_x} e^{ik_x} s_{k_x}^{(n)} e^{ik_x x} dk_x \\ \int_{k_x} e^{-ik_x} p_{k_x}^{(n)} e^{ik_x x} dk_x \end{bmatrix} \quad \text{(S20)}$$

This equation can be used to solve the Fourier transforms as functions of the time step. In the following subsections, we solve this equation for two cases of no phase modulation as well as time dependent linear phase modulation.

A. Zero phase modulation:

For the case of no applied phase, we have:

$$\begin{bmatrix} s_{k_x}^{(n+1)} \\ p_{k_x}^{(n+1)} \end{bmatrix} = \frac{1}{\sqrt{2}} \begin{bmatrix} e^{ik_x} & e^{-ik_x} \\ -e^{ik_x} & e^{-ik_x} \end{bmatrix} \begin{bmatrix} s_{k_x}^{(n)} \\ p_{k_x}^{(n)} \end{bmatrix} \quad \text{(S21)}$$

Note that the evolution matrix has the determinant of 1. Based on this matrix, the effective Hamiltonian, $H_{eff} = i \log(U)$, is given by:

$$H = \frac{\arccos\left(\cos(k_x)/\sqrt{2}\right)}{\sqrt{2}\sin\left(\arccos\left(\cos(k_x)/\sqrt{2}\right)\right)} \times \begin{pmatrix} \sin(k_x) & -ie^{-ik_x} \\ ie^{ik_x} & -\sin(k_x) \end{pmatrix} \quad \text{(S22)}$$

The obtained Hamiltonian is hermitian and its eigenvalues are given by:

$$E_{\pm} = \pm \arccos\left(\cos(k_x)/\sqrt{2}\right) \quad \text{(S23)}$$

The evolution after n steps is given by:

$$\begin{bmatrix} s_{k_x}^{(n)} \\ p_{k_x}^{(n)} \end{bmatrix} = \frac{1}{\sqrt{2^n}} \begin{bmatrix} e^{ik_x} & e^{-ik_x} \\ -e^{ik_x} & e^{-ik_x} \end{bmatrix}^n \begin{bmatrix} s_{k_x}^{(0)} \\ p_{k_x}^{(0)} \end{bmatrix} \quad \text{(S24)}$$

Assuming that the whole evolution is caused by a single pulse at the origin ($U_x^{(0)} = \delta(x)$, $D_x^{(0)} = 0$ which is equivalent to $S_x^{(0)} = \delta(x)$, $P_x^{(0)} = \delta(x)$), we have:

$$\begin{bmatrix} s_{k_x}^{(0)} \\ p_{k_x}^{(0)} \end{bmatrix} = \begin{bmatrix} 1 \\ 1 \end{bmatrix} \tag{S25}$$

Therefore, for the down channel pulses, $d_{k_x}^{(n)} = 0.5\left(s_{k_x}^{(n)} - p_{k_x}^{(n)}\right)$, we have:

$$d_{k_x}^{(n)} = \frac{e^{ik_x}}{\sqrt{2}} \frac{\sin\left(n \arccos\left(\cos\left(k_x\right)/\sqrt{2}\right)\right)}{\sin\left(\arccos\left(\cos\left(k_x\right)/\sqrt{2}\right)\right)} \tag{S26}$$

All the moments, such as the distribution variances and averages ($\langle x^2\rangle_D$ and $\langle x\rangle_D$) as functions of the time step n, can be obtained from the above expression.

Based on the fact that:

$$d_{k_x}^{(n)} = \sum_x D_x^{(n)} e^{-ik_x x} \tag{S27}$$

Then:

$$d_{l_x}^{(n)*} d_{k_x}^{(n)} = \sum_p \sum_x e^{-i(k_x x - l_x p)} D_p^{(n)*} D_x^{(n)} \tag{S28}$$

Therefore, the following equations can be obtained straightforwardly:

$$\begin{aligned} P_D &= \sum_x \left|D_x^{(n)}\right|^2 = \frac{1}{2\pi}\int_{k_x=0}^{2\pi} \left|d_{k_x}^{(n)}\right|^2 dk_x \\ &= \frac{1}{4\pi}\int_{k_x=0}^{2\pi} \frac{\sin^2\left(n \arccos\left(\cos\left(k_x\right)/\sqrt{2}\right)\right)}{\sin^2\left(\arccos\left(\cos\left(k_x\right)/\sqrt{2}\right)\right)} dk_x \end{aligned} \tag{S29}$$

$$\langle x\rangle_D = \sum_x x\left|D_x^{(n)}\right|^2 = \frac{1}{2\pi}\int_{k_x=0}^{2\pi} d_{k_x}^{(n)*}\left(i\frac{d}{dk_x}\right) d_{k_x}^{(n)} dk_x \tag{S30}$$

$$\begin{aligned} \left\langle x^2\right\rangle_D &= \sum_x x^2\left|D_x^{(n)}\right|^2 \\ &= \frac{1}{2\pi}\int_{k_x=0}^{2\pi} d_{k_x}^{(n)*}\left(i\frac{d}{dk_x}\right)^2 d_{k_x}^{(n)} dk_x \end{aligned} \tag{S31}$$

In the limit of large n, we have:

$$P_D \to \frac{1}{8\pi}\int_{k_x=0}^{2\pi} \frac{1}{1-\cos^2\left(k_x\right)/2} dk_x = \frac{1}{2\sqrt{2}} \tag{S32}$$

$$\langle x\rangle_D \to 0 \tag{S33}$$

$$\left\langle x^2\right\rangle_D \to \frac{n^2}{16\pi}\int_{k_x=0}^{2\pi} \frac{\sin^2\left(k_x\right)}{\left(1-\cos^2\left(k_x\right)/2\right)^2} dk_x = \frac{n^2}{8\sqrt{2}} \tag{S34}$$

These results prove that the spatial quadratic mean of the quantum walk distribution varies linearly with the time step. Note that these average values are normalized relative to the total power in the up and down channels. However, they can also be normalized relative to the total power present in the corresponding channel. Since the probabilities of P_D and P_U tend toward constant values, by the latter normalization the asymptotic behavior of the quadratic mean remains linear relative to the time step.

Similarly, we can investigate the up channel:

$$\begin{aligned} u_{k_x}^{(n)} &= 0.5\left(s_{k_x}^{(n)} + p_{k_x}^{(n)}\right) \\ &= \cos\left(n \arccos\left(\cos\left(k_x\right)/\sqrt{2}\right)\right) \\ &\quad - i\frac{\sin\left(k_x\right)}{\sqrt{2}} \frac{\sin\left(n \arccos\left(\cos\left(k_x\right)/\sqrt{2}\right)\right)}{\sin\left(\arccos\left(\cos\left(k_x\right)/\sqrt{2}\right)\right)} \end{aligned} \tag{S35}$$

$$\begin{aligned} P_U &= \sum_x \left|U_x^{(n)}\right|^2 = \frac{1}{2\pi}\int_{k_x=0}^{2\pi} \left|u_{k_x}^{(n)}\right|^2 dk_x \\ &= \frac{1}{4\pi}\int_{k_x=0}^{2\pi} \sin^2\left(k_x\right) \frac{\sin^2\left(n \arccos\left(\cos\left(k_x\right)/\sqrt{2}\right)\right)}{\sin^2\left(\arccos\left(\cos\left(k_x\right)/\sqrt{2}\right)\right)} dk_x \\ &\quad + \frac{1}{2\pi}\int_{k_x=0}^{2\pi} \cos^2\left(n \arccos\left(\cos\left(k_x\right)/\sqrt{2}\right)\right) dk_x \end{aligned} \tag{S36}$$

$$\langle x\rangle_U = \sum_x x\left|U_x^{(n)}\right|^2 = \frac{1}{2\pi}\int_{k_x=0}^{2\pi} u_{k_x}^{(n)*}\left(i\frac{d}{dk_x}\right) u_{k_x}^{(n)} dk_x \tag{S37}$$

$$\begin{aligned} \left\langle x^2\right\rangle_U &= \sum_x x^2\left|U_x^{(n)}\right|^2 \\ &= \frac{1}{2\pi}\int_{k_x=0}^{2\pi} u_{k_x}^{(n)*}\left(i\frac{d}{dk_x}\right)^2 u_{k_x}^{(n)} dk_x \end{aligned} \tag{S38}$$

In the limit of large n, we have:

$$P_U \to \frac{1}{2} + \frac{1}{8\pi}\int_{k_x=0}^{2\pi} \frac{\sin^2\left(k_x\right)}{1-\cos^2\left(k_x\right)/2} dk_x = 1 - \frac{1}{2\sqrt{2}} \tag{S39}$$

$$\langle x\rangle_U \to \left(1 - \frac{\sqrt{2}}{2}\right) n \tag{S40}$$

$$\begin{aligned} \left\langle x^2\right\rangle_U &\to \frac{n^2}{8\pi}\int_{k_x=0}^{2\pi} \frac{\sin^2\left(k_x\right)\left(\sin^2\left(k_x\right)+\frac{1}{2}\right)}{\left(1-\frac{\cos^2\left(k_x\right)}{2}\right)^2} dk_x \\ &= \left(1 - \frac{9}{8\sqrt{2}}\right) n^2 \end{aligned} \tag{S41}$$

B. Time-dependent phase modulation:

For the case of a time-dependent but coordinate-independent phase modulation, we have:

$$\begin{bmatrix} s_{k_x}^{(n+1)} \\ p_{k_x}^{(n+1)} \end{bmatrix} = \begin{bmatrix} \frac{e^{i(k_x+\phi_n)}}{\sqrt{2}} & \frac{e^{-i(k_x+\phi_n)}}{\sqrt{2}} \\ -\frac{e^{i(k_x+\phi_n)}}{\sqrt{2}} & \frac{e^{-i(k_x+\phi_n)}}{\sqrt{2}} \end{bmatrix} \begin{bmatrix} s_{k_x}^{(n)} \\ p_{k_x}^{(n)} \end{bmatrix} \tag{S42}$$

We consider phase modulations that are linearly varying with the time step, such that $\phi_n = n\phi$. Therefore, by defining $w_{k_x}^{(n)} = s_{k_x-n\phi}^{(n)}$ and $v_{k_x}^{(n)} = p_{k_x-n\phi}^{(n)}$:

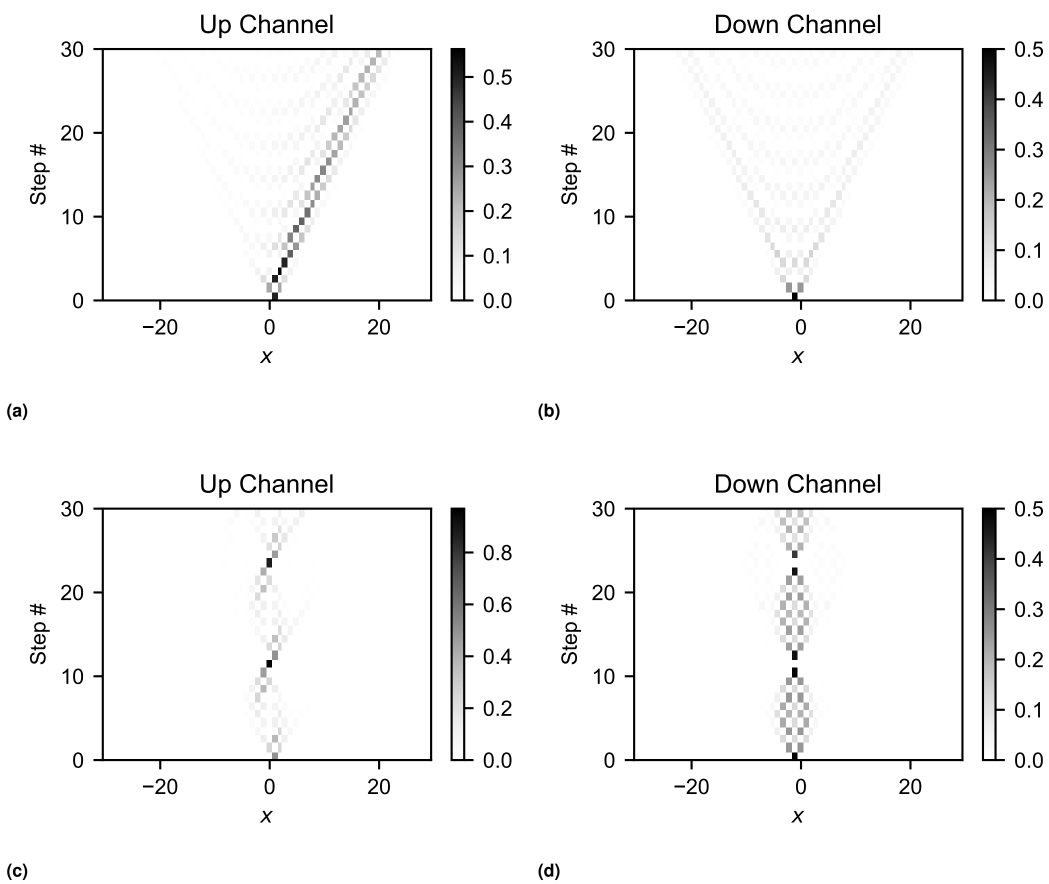

Fig. S3. The quantum walk probability distribution in the (a) up and (b) down channels at different time steps under no applied gauge field. The quantum walk probability distribution in the (c) up and (d) down channels at different time steps under a time-varying gauge field with a phase of $\phi = \pi/6$. Under the presence of a nonzero phase, the walker returns back to the origin after a fixed number of steps, which is determined by the applied phase.

$$\begin{bmatrix} w_{k_x+\phi}^{(n+1)} \\ v_{k_x+\phi}^{(n+1)} \end{bmatrix} = \frac{1}{\sqrt{2}} \begin{bmatrix} e^{ik_x} & e^{-ik_x} \\ -e^{ik_x} & e^{-ik_x} \end{bmatrix} \begin{bmatrix} w_{k_x}^{(n)} \\ v_{k_x}^{(n)} \end{bmatrix} \tag{S43}$$

The evolution matrix can be obtained for rational values of phase modulations, $\phi/2\pi = p/q$. We then can obtain the pseudo-energy band diagrams from the evolution matrix. In the following, we obtain the eigen-energies for any rational value of phase modulation, straightforwardly.

By defining $r_{k_x}^{(n)} = \begin{bmatrix} w_{k_x}^{(n)} & v_{k_x}^{(n)} \end{bmatrix}^T$ and

$$\begin{aligned} M_{k_x} &= \frac{1}{\sqrt{2}} \begin{bmatrix} e^{ik_x} & e^{-ik_x} \\ -e^{ik_x} & e^{-ik_x} \end{bmatrix} \\ &= \frac{1}{\sqrt{2}} \begin{bmatrix} 1 & 1 \\ -1 & 1 \end{bmatrix} \begin{bmatrix} e^{ik_x} & 0 \\ 0 & e^{-ik_x} \end{bmatrix}, \end{aligned} \tag{S44}$$

we have:

$$r_{k_x+\phi}^{(n+1)} = M_{k_x} r_{k_x}^{(n)} \tag{S45}$$

After q steps, we have:

$$r_{k_x}^{(n+q)} = M_{k_x+(q-1)\phi} \dots M_{k_x} r_{k_x}^{(n)} \tag{S46}$$

Therefore, by defining $Y_{k_x}^{(i)} = M_{k_x+(i-1)\phi} \dots M_{k_x}$, the following holds:

$$M_{k_x} = \frac{1}{\sqrt{2}} \begin{bmatrix} e^{ik_x} & e^{-ik_x} \\ -e^{ik_x} & e^{-ik_x} \end{bmatrix} \tag{S47}$$

$$r_{k_x}^{(n+q)} = Y_{k_x}^{(q)} r_{k_x}^{(n)} \tag{S48}$$

Since M and Y are unitary matrices, the following equations hold for the eigen-energies:

$$Y_{k_x}^{(q)} r_{k_x}^{(n)} = e^{iqE} r_{k_x}^{(n)} \tag{S49}$$

$$Y_{k_x}^{(q)\dagger} r_{k_x}^{(n)} = e^{-iqE} r_{k_x}^{(n)} \tag{S50}$$

Consequently, we have:

$$\frac{1}{2}\left(Y_{k_x}^{(q)} + Y_{k_x}^{(q)\dagger}\right) r_{k_x}^{(n)} = \cos(qE)\, r_{k_x}^{(n)} \tag{S51}$$

It can be verified that not only for $\phi = 2\pi/q$ but also for any $\phi = 2\pi p/q$, with q and p being relatively prime, the following holds:

$$\begin{aligned} \frac{1}{2}\left(Y_{k_x}^{(q)} + Y_{k_x}^{(q)\dagger}\right) &= \left(\cos\left(\frac{\pi q}{2}\right) - \cos(qk_x)\right) \frac{(-1)^q}{\sqrt{2^q}} I \\ &\quad - \cos\left(\frac{\pi q}{2}\right) I \end{aligned} \tag{S52}$$

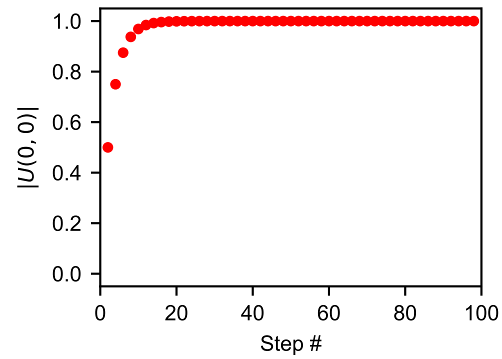

(a)

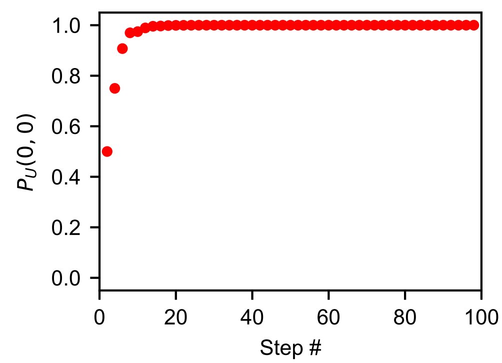

(b)

Fig. S4. (a) The probability amplitude of the quantum walker to be at the origin in the up channel after q steps as a function of q. (b) The normalized probability of the quantum walker to return to the origin in the up channel after q steps as a function of q.

Therefore, the eigen-energies are given by

$$\begin{aligned} E_{n,\pm,k_x} = \frac{2n\pi}{q} \pm \frac{1}{q} \arccos \Big[&\left(\cos\left(\frac{\pi q}{2}\right) - \cos(qk_x)\right) \\ \times \frac{(-1)^q}{\sqrt{2^q}} &- \cos\left(\frac{\pi q}{2}\right) \Big], \end{aligned} \tag{S53}$$

which explicitly expresses the eigen-energies for any of $2q$ bands.

Based on this analytical expression for the allowed energies, it can be verified that the bandgap does not exist for any rational value of phase modulation.

Since we are interested in the evolution of the quantum walk after q steps, we obtain the following for any $k_x = \frac{\pi}{2} + \frac{2\pi m}{q}$ with $m \in \mathbb{Z}$:

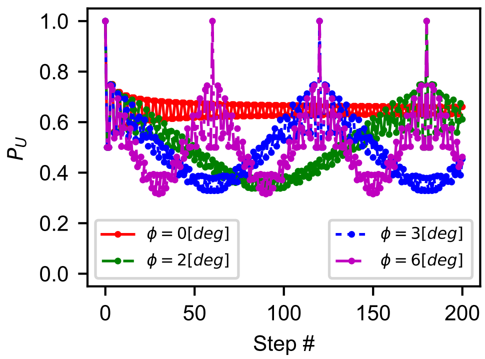

(a)

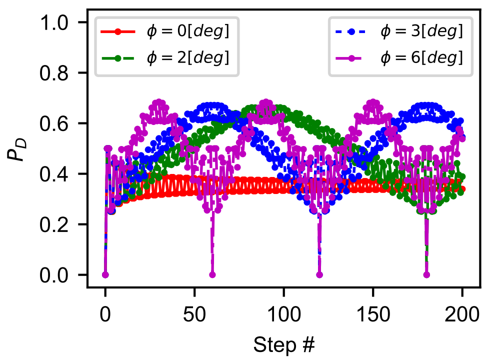

(b)

Fig. S5. (a) The total probability of the quantum walker to be in the up channel and (b) down channel as a function of the time step for different values of phase modulations.

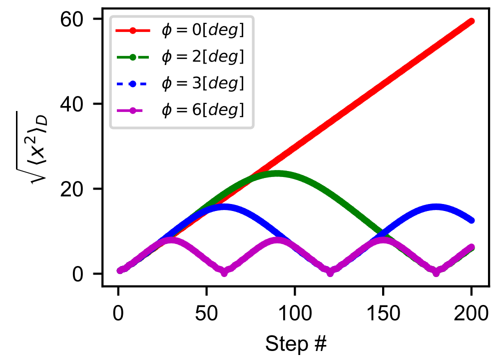

(a)

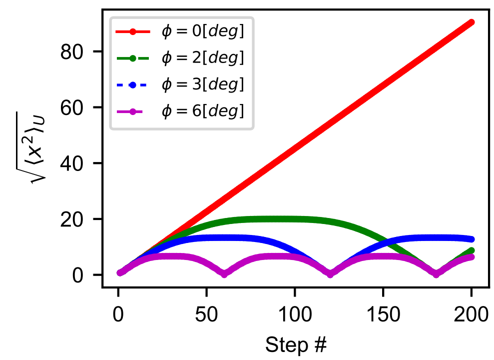

(b)

Fig. S6. The quadratic mean of x for the (a) down channel and (b) up channel as a function of the time step for different values of phase modulations.

$$\begin{aligned} &qE_{n,\pm,k_x} \\ &= \pm \arccos\left[\left(\cos\left(\frac{\pi q}{2}\right) - \cos\left(qk_x\right)\right)\frac{(-1)^q}{\sqrt{2^q}} - \cos\left(\frac{\pi q}{2}\right)\right] \\ &= \begin{cases} \pi: & q = 4g \\ \pm\pi/2: & q = 4g+1 \\ 0: & q = 4g+2 \\ \pm\pi/2: & q = 4g+3 \end{cases}, \end{aligned} \tag{S54}$$

which corresponds to:

$$e^{-iqE_{n,\pm,k_x}} = \begin{cases} -1: & q = 4g \\ \mp i: & q = 4g+1 \\ 1: & q = 4g+2 \\ \mp i: & q = 4g+3 \end{cases}. \tag{S55}$$

We can express any amplitude ψ representing the up channel $U(x,n)$ or the down channel $D(x,n)$ in terms of the initial conditions as:

$$\psi\left(k_x, n\right) = \sum_{j=1}^{2q} e^{-iE_{j,k_x}n} A_{j,k_x} \tag{S56}$$

Therefore, based on the above expressions, such an amplitude is expressed after q steps for even values of q via:

$$\psi\left(k_x, q\right) = s\sum_{j=1}^{2q} e^{ik_x x} A_{j,k_x} = s\psi\left(k_x, 0\right), \tag{S57}$$

in which

$$s = \begin{cases} -1: & q = 4g \\ +1: & q = 4g+2 \end{cases}. \tag{S58}$$

This equality holds for any $k_x = \frac{\pi}{2} + \frac{2\pi m}{q}$ with $m \in \mathbb{Z}$ and for other values of k_x it holds by approximation. However, with the increase of q, the approximation becomes more and more accurate. Therefore, the following approximation holds, and it becomes exact in the limit of $q \to \infty$:

$$\psi\left(x, q\right) \cong s\psi\left(x, 0\right). \tag{S59}$$

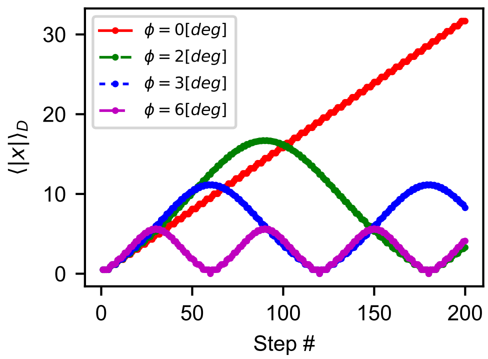

(a)

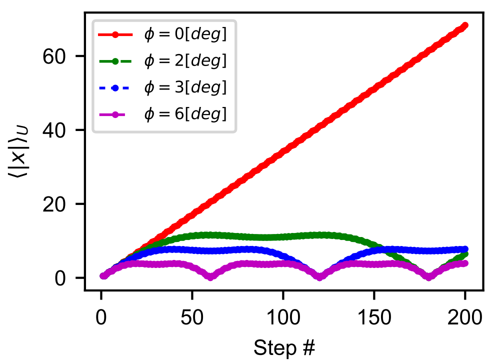

(b)

Fig. S7. The norm one of x for the (a) down channel and (b) up channel as a function of the time step for different values of phase modulations.

This proves that revival happens after q steps ($|\psi(x,q)| \cong |\psi(x,0)|$) for even values of q and it becomes more accurate with the increase of q. The variations of the quantum walk probability distribution as a function of the time step under no applied gauge field as well as a linearly time varying gauge field with $\phi = \pi/6$ are shown in Fig. S3. This figure clearly shows the revival caused by Bloch oscillations under the time varying gauge field.

Since we start with a unity pulse at the origin in the up channel, we can plot the probability amplitude of the quantum walker to be at the origin after q steps. We have plotted this amplitude in Fig. S4a. This figure confirms the fact that with the increase of q, the quantum walker indeed becomes more localized at the origin and the corresponding probability tends toward unity in the limit of $q \to \infty$. The corresponding normalized probability of the quantum walker to return to the origin after q steps is also shown in Fig. S4b.

We can also consider the total probability of the quantum walker to be in the up channel or down channel as a function of the time step. We have plotted these probabilities in Fig. S5 for different values of phase modulations. As we expect, the probability of the quantum walker to be in the up channel is close to one after $2\pi/\phi$ time steps. It is interesting to note that the minimum value of the probability of the quantum walker to be in the up channel is not zero and instead it is close to $1/2\sqrt{2}$. The probability in the up channel reaches this value after around π/ϕ time steps.

Figures S6a and S6b summarize the numerical results for the variation of $\sqrt{\langle x^2\rangle_D}$ and $\sqrt{\langle x^2\rangle_U}$ with the time step for different values of ϕ. The obtained results show that for $1 \ll n \ll \pi/\phi$, $\sqrt{\langle x^2\rangle_D}$ varies as $n/\sqrt{8\sqrt{2}}$ as one would expect from the zero-phase modulation case. Moreover, the numerical results show that for small values of ϕ, $\sqrt{\langle x^2\rangle_D}$ reaches the maximum value at $n \cong \pi/\phi$. These results also show that $\langle x^2\rangle_D$ tends toward zero at $n \cong 2\pi/\phi$, which is consistent with the above analysis. In addition to the quadratic means, we can also look at the variations in the norm ones of the quantum walk distributions. Figures S7a and S7b summarize the numerical results for the variation of $\langle|x|\rangle_D$ and $\langle|x|\rangle_U$ with the time step for different values of ϕ.

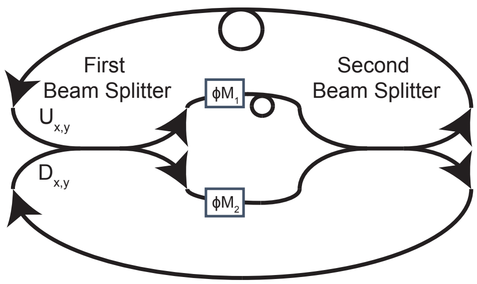

Fig. S8. Simplified version of the schematic of a two-dimensional quantum random walk setup

3. THEORETICAL ANALYSIS FOR TWO-DIMENSIONAL QUANTUM RANDOM WALKS:

In this section, we generalize the concepts that are presented in the previous section to two-dimensional quantum random walks. By assuming that all the losses in the setup are fully compensated by the amplifiers and all the polarization changes are compensated by polarization controllers, the setup can be represented as an ideal setup, as shown in Fig. S8. We have demonstrated in our earlier work how pulses will propagate under arbitrary phase modulation patterns [1]. By representing the pulses that exist at time step n by $U_{x,y}^{(n)}$ and $D_{x,y}^{(n)}$ in the up and down channels, respectively, we have shown the evolution of the pulses obey the following equations:

$$U_{x,y}^{(n+1)} = \frac{e^{i\phi_{n,y-1}}}{2}\left(U_{x+1,y-1}^{(n)} - D_{x+1,y-1}^{(n)}\right) - \frac{e^{-i\phi_{n,y-1}}}{2}\left(U_{x-1,y-1}^{(n)} + D_{x-1,y-1}^{(n)}\right) \tag{S60}$$

$$D_{x,y}^{(n+1)} = \frac{e^{i\phi_{n,y+1}}}{2}\left(U_{x+1,y+1}^{(n)} - D_{x+1,y+1}^{(n)}\right) + \frac{e^{-i\phi_{n,y+1}}}{2}\left(U_{x-1,y+1}^{(n)} + D_{x-1,y+1}^{(n)}\right) \tag{S61}$$

By defining $S_{x,y}^{(n)} = U_{x,y}^{(n)} + D_{x,y}^{(n)}$ and $P_{x,y}^{(n)} = U_{x,y}^{(n)} - D_{x,y}^{(n)}$, the obtained equations can be written as:

$$\begin{bmatrix} S_{x,y}^{(n+1)} \\ P_{x,y}^{(n+1)} \end{bmatrix} = \frac{1}{2}\begin{bmatrix} e^{-i\phi_{n,y+1}} & e^{i\phi_{n,y+1}} & -e^{-i\phi_{n,y-1}} & e^{i\phi_{n,y-1}} \\ -e^{-i\phi_{n,y+1}} & -e^{i\phi_{n,y+1}} & -e^{-i\phi_{n,y-1}} & e^{i\phi_{n,y-1}} \end{bmatrix} \times \begin{bmatrix} S_{x-1,y+1}^{(n)} \\ P_{x+1,y+1}^{(n)} \\ S_{x-1,y-1}^{(n)} \\ P_{x+1,y-1}^{(n)} \end{bmatrix} \tag{S62}$$

By defining $s_{k_x,k_y}^{(n)}$ and $p_{k_x,k_y}^{(n)}$ as Fourier transforms of $S_{x,y}^{(n)}$ and $P_{x,y}^{(n)}$, we have:

$$\begin{bmatrix} S_{x,y}^{(n)} \\ P_{x,y}^{(n)} \end{bmatrix} = \frac{1}{4\pi^2}\begin{bmatrix} \int\int_{k_x,k_y} s_{k_x,k_y}^{(n)} e^{ik_x x+ik_y y} dk_x dk_y \\ \int\int_{k_x,k_y} p_{k_x,k_y}^{(n)} e^{ik_x x+ik_y y} dk_x dk_y \end{bmatrix} \tag{S63}$$

Therefore:

$$\begin{bmatrix} \int\int_{k_x,k_y} s_{k_x,k_y}^{(n+1)} e^{ik_x x+ik_y y} dk_x dk_y \\ \int\int_{k_x,k_y} p_{k_x,k_y}^{(n+1)} e^{ik_x x+ik_y y} dk_x dk_y \end{bmatrix} = \frac{1}{2}\begin{bmatrix} e^{-i\phi_{n,y+1}} & e^{i\phi_{n,y+1}} & -e^{-i\phi_{n,y-1}} & e^{i\phi_{n,y-1}} \\ -e^{-i\phi_{n,y+1}} & -e^{i\phi_{n,y+1}} & -e^{-i\phi_{n,y-1}} & e^{i\phi_{n,y-1}} \end{bmatrix} \times \begin{bmatrix} \int\int_{k_x,k_y} e^{ik_y-ik_x} s_{k_x,k_y}^{(n)} e^{ik_x x+ik_y y} dk_x dk_y \\ \int\int_{k_x,k_y} e^{ik_x+ik_y} p_{k_x,k_y}^{(n)} e^{ik_x x+ik_y y} dk_x dk_y \\ \int\int_{k_x,k_y} e^{-ik_x-ik_y} s_{k_x,k_y}^{(n)} e^{ik_x x+ik_y y} dk_x dk_y \\ \int\int_{k_x,k_y} e^{ik_x-ik_y} p_{k_x,k_y}^{(n)} e^{ik_x x+ik_y y} dk_x dk_y \end{bmatrix} \tag{S64}$$

This equation can be used to solve the Fourier transforms as functions of the time step. The evolution for the case of no phase modulation has already been investigated [1]. Here we focus on the case in which we apply a phase modulation that varies linearly with the time step.

A. Time-dependent phase modulation:

For the case of a time-dependent but coordinate-independent phase modulation, we have:

$$\begin{bmatrix} s_{k_x,k_y}^{(n+1)} \\ p_{k_x,k_y}^{(n+1)} \end{bmatrix} = \begin{bmatrix} ie^{-i(k_x+\phi_n)}\sin(k_y) & e^{i(k_x+\phi_n)}\cos(k_y) \\ -e^{-i(k_x+\phi_n)}\cos(k_y) & -ie^{i(k_x+\phi_n)}\sin(k_y) \end{bmatrix} \times \begin{bmatrix} s_{k_x,k_y}^{(n)} \\ p_{k_x,k_y}^{(n)} \end{bmatrix} \tag{S65}$$

Therefore, by defining $w_{k_x,k_y}^{(n)} = s_{k_x-n\phi,k_y}^{(n)}$ and $v_{k_x,k_y}^{(n)} = p_{k_x-n\phi,k_y}^{(n)}$:

$$\begin{bmatrix} w_{k_x+\phi,k_y}^{(n+1)} \\ v_{k_x+\phi,k_y}^{(n+1)} \end{bmatrix} = \begin{bmatrix} ie^{-ik_x}\sin(k_y) & e^{ik_x}\cos(k_y) \\ -e^{-ik_x}\cos(k_y) & -ie^{ik_x}\sin(k_y) \end{bmatrix} \times \begin{bmatrix} w_{k_x,k_y}^{(n)} \\ v_{k_x,k_y}^{(n)} \end{bmatrix} \tag{S66}$$

Using this equation, we can obtain a propagation matrix for rational values of phase modulations, $\phi/2\pi = p/q$. In the following, we obtain the eigen-energies for any rational value of phase modulation, straightforwardly.

By defining $r_{k_x,k_y}^{(n)} = \begin{bmatrix} w_{k_x,k_y}^{(n)} & v_{k_x,k_y}^{(n)} \end{bmatrix}^T$ and

$$M_{k_x,k_y} = \begin{bmatrix} ie^{-ik_x}\sin(k_y) & e^{ik_x}\cos(k_y) \\ -e^{-ik_x}\cos(k_y) & -ie^{ik_x}\sin(k_y) \end{bmatrix}, \tag{S67}$$

we have:

$$r_{k_x+\phi,k_y}^{(n+1)} = M_{k_x,k_y} r_{k_x,k_y}^{(n)} \tag{S68}$$

After q steps, we have:

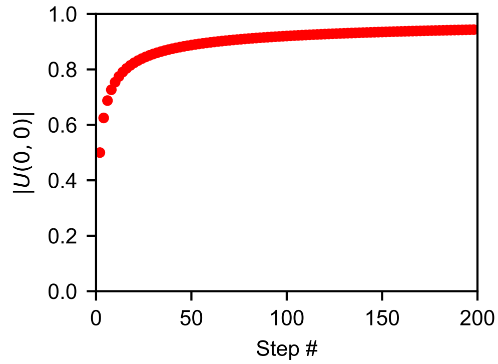

(a)

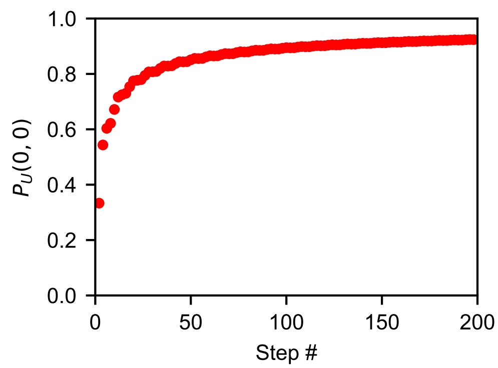

(b)

Fig. S9. (a) The probability amplitude of the quantum walker to be at the origin in the up channel after q steps as a function of q. (b) The normalized probability of the quantum walker to return to the origin in the up channel after q steps as a function of q.

$$r_{k_x,k_y}^{(n+q)} = M_{k_x+(q-1)\phi,k_y} \dots M_{k_x,k_y} r_{k_x,k_y}^{(n)} \tag{S69}$$

Therefore, by defining $Y_{k_x,k_y}^{(i)} = M_{k_x+(i-1)\phi,k_y} \dots M_{k_x,k_y}$, the following holds:

$$r_{k_x,k_y}^{(n+q)} = Y_{k_x,k_y}^{(q)} r_{k_x,k_y}^{(n)} \tag{S70}$$

Since M and Y are unitary matrices, the following equations hold for the eigen-energies:

$$Y_{k_x,k_y}^{(q)} r_{k_x,k_y}^{(n)} = e^{iqE} r_{k_x,k_y}^{(n)} \tag{S71}$$

$$Y_{k_x,k_y}^{(q)\dagger} r_{k_x,k_y}^{(n)} = e^{-iqE} r_{k_x,k_y}^{(n)} \tag{S72}$$

Consequently, we have:

$$\frac{1}{2}\left(Y_{k_x,k_y}^{(q)} + Y_{k_x,k_y}^{(q)\dagger}\right) r_{k_x,k_y}^{(n)} = \cos\left(qE\right) r_{k_x,k_y}^{(n)} \tag{S73}$$

It can be verified that not only for $\phi = 2\pi/q$ but also for any $\phi = 2\pi p/q$, with q and p being relatively prime, the following holds:

$$\begin{aligned}\frac{1}{2}\left(Y_{k_x,k_y}^{(q)} + Y_{k_x,k_y}^{(q)\dagger}\right) = \left(\cos\left(\frac{\pi q}{2}\right) - \cos\left(qk_x + \frac{\pi q}{2}\right)\right)\sin^q\left(k_y\right) I \\ - \cos\left(\frac{\pi q}{2}\right) I\end{aligned} \tag{S74}$$

Therefore, the eigen-energies are given by

$$\begin{aligned}E_{n,\pm,k_x,k_y} = \frac{2n\pi}{q} \pm \frac{1}{q}\arccos\Big[\left(\cos\left(\frac{\pi q}{2}\right) - \cos\left(qk_x + \frac{\pi q}{2}\right)\right) \\ \times \sin^q\left(k_y\right) - \cos\left(\frac{\pi q}{2}\right)\Big],\end{aligned} \tag{S75}$$

which explicitly expresses the eigen-energies for any of $2q$ bands.

Based on this analytical expression for the allowed energies, it can be verified that the bandgap does not exist for any rational value of phase modulation. The energy band diagrams for $\phi = \pi/2$, $\phi = \pi/3$, and $\phi = \pi/4$ have been plotted in Fig. 2 of the main text.

Since we are interested in the evolution of the quantum walk after q steps, we obtain the following for any $k_x = \frac{2\pi m}{q}$ with $m \in \mathbb{Z}$:

$$\begin{aligned}&qE_{n,\pm,k_x,k_y} \\ &= \pm\arccos\left[\left(\cos\left(\frac{\pi q}{2}\right) - \cos\left(qk_x + \frac{\pi q}{2}\right)\right)\sin^q\left(k_y\right) - \cos\left(\frac{\pi q}{2}\right)\right] \\ &= \begin{cases}\pi: & q = 4g \\ \pm\pi/2: & q = 4g+1 \\ 0: & q = 4g+2 \\ \pm\pi/2: & q = 4g+3\end{cases},\end{aligned} \tag{S76}$$

which corresponds to:

$$e^{-iqE_{n,\pm,k_x,k_y}} = \begin{cases}-1: & q = 4g \\ \mp i: & q = 4g+1 \\ 1: & q = 4g+2 \\ \mp i: & q = 4g+3\end{cases}. \tag{S77}$$

We can express any amplitude ψ representing the up channel $U(x,y,n)$ or the down channel $D(x,y,n)$ in terms of the initial conditions as:

$$\psi\left(k_x,y,n\right) = \sum_{j=1}^{2q}\int_{k_y} e^{-iE_{j,k_x,k_y}n} e^{ik_y y} A_{j,k_x,k_y} dk_y \tag{S78}$$

Therefore, based on the above expressions, such an amplitude is expressed after q steps for even values of q via:

$$\psi\left(k_x,y,q\right) = s\sum_{j=1}^{2q}\int_{k_y} e^{ik_y y} A_{j,k_x,k_y} dk_y = s\psi\left(k_x,y,0\right), \tag{S79}$$

in which

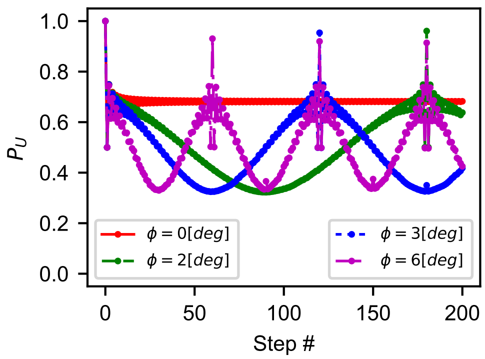

(a)

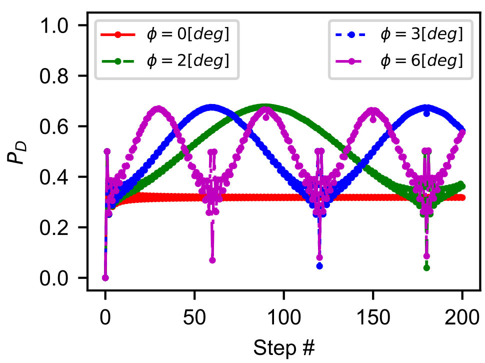

(b)

Fig. S10. (a) The total probability of the quantum walker to be in the up channel and (b) the total probability of the quantum walker to be in the down channel as a function of the time step for different values of phase modulations.

$$s = \begin{cases} -1: & q = 4g \\ +1: & q = 4g+2 \end{cases}. \tag{S80}$$

This equality holds for any $k_x = \frac{2\pi m}{q}$ with $m \in \mathbb{Z}$ and for other values of k_x it holds by approximation. However, with the increase of q, the approximation becomes more and more accurate. Therefore, the following approximation holds, and it becomes exact in the limit of $q \to \infty$:

$$\psi(x, y, q) \cong s\psi(x, y, 0). \tag{S81}$$

This proves that revival (caused by Bloch oscillations) happens after q steps ($|\psi(x, y, q)| \cong |\psi(x, y, 0)|$) for even values of q and it becomes more accurate with the increase of q.

Since we start with a unity pulse at the origin in the up channel, we can plot the probability amplitude of the quantum walker to be at the origin after q steps. We have plotted this amplitude in Fig. S9a. This figure confirms the fact that with the increase of q, the quantum walker indeed becomes more trapped at the origin and the corresponding probability tends toward unity in the limit of $q \to \infty$. The corresponding normalized probability of the quantum walker to return to the origin after q steps is also shown in Fig. S9b.

We can also consider the total probability of the quantum walker to be in the up channel or down channel as a function of the time step. We have plotted these probabilities in Fig. S10 for different values of phase modulations. As we expect, the probability of the quantum walker to be in the up channel is close to one after $2\pi/\phi$ time steps. The minimum value of the probability of the quantum walker to be in the up channel is not zero and instead it is close to $1/\pi$. The probability in the up channel reaches this value after around π/ϕ time steps.

We can also analyze the transient variation of the quantum walk. For this purpose, the obtained propagation equation for $w_{k_x,k_y}^{(n)}$ and $v_{k_x,k_y}^{(n)}$ can be transformed to the following equation:

$$\begin{aligned} &\begin{bmatrix} w_{k_x,k_y}^{(n+1)} + v_{k_x,k_y}^{(n+1)} \\ w_{k_x,k_y}^{(n+1)} - v_{k_x,k_y}^{(n+1)} \end{bmatrix} \\ &= \begin{bmatrix} ie^{-ik_y} \sin(k_x - \phi) & -e^{-ik_y} \cos(k_x - \phi) \\ e^{ik_y} \cos(k_x - \phi) & -ie^{ik_y} \sin(k_x - \phi) \end{bmatrix} \\ &\times \begin{bmatrix} w_{k_x-\phi,k_y}^{(n)} + v_{k_x-\phi,k_y}^{(n)} \\ w_{k_x-\phi,k_y}^{(n)} - v_{k_x-\phi,k_y}^{(n)} \end{bmatrix} \end{aligned} \tag{S82}$$

Focusing on the down channel, we know that at time step n, we have:

$$\begin{aligned} d_{k_x,k_y}^{(n)} &= 0.5\left(s_{k_x,k_y}^{(n)} - p_{k_x,k_y}^{(n)}\right) \\ &= 0.5\left(w_{k_x+n\phi,k_y}^{(n)} - v_{k_x+n\phi,k_y}^{(n)}\right) \end{aligned} \tag{S83}$$

From this expression, we can obtain the following equation for $\langle y^2 \rangle_D$:

$$\begin{aligned} &\left\langle y^2 \right\rangle_D = \sum_{x,y} y^2 \left| D_{x,y}^{(n)} \right|^2 \\ &= \frac{1}{4\pi^2} \int_{k_y=0}^{2\pi} \int_{k_x=0}^{2\pi} d_{k_x,k_y}^{(n)*} \left(i\frac{d}{dk_y} \right)^2 d_{k_x,k_y}^{(n)} dk_x dk_y \\ &= \frac{1}{16\pi^2} \int_{k_y=0}^{2\pi} \int_{k_x=0}^{2\pi} \left(w_{k_x,k_y}^{(n)} - v_{k_x,k_y}^{(n)} \right)^* \\ &\times \left(i\frac{d}{dk_y} \right)^2 \left(w_{k_x,k_y}^{(n)} - v_{k_x,k_y}^{(n)} \right) dk_x dk_y \end{aligned} \tag{S84}$$

Therefore, it is enough to obtain $w_{k_x,k_y}^{(n)} - v_{k_x,k_y}^{(n)}$ at time step n in order to calculate the statistics of the quantum walk. Contrary to the zero-phase modulation, in which propagation matrices remain constant through time, here the evolution can be explained in terms of the product of n matrices, which are not necessarily equal to each other:

$$\begin{aligned} &\begin{bmatrix} 0.5\left(w_{k_x,k_y}^{(n)} + v_{k_x,k_y}^{(n)} \right) \\ 0.5\left(w_{k_x,k_y}^{(n)} - v_{k_x,k_y}^{(n)} \right) \end{bmatrix} \\ &= \begin{bmatrix} ie^{-ik_y} \sin(k_x - \phi) & -e^{-ik_y} \cos(k_x - \phi) \\ e^{ik_y} \cos(k_x - \phi) & -ie^{ik_y} \sin(k_x - \phi) \end{bmatrix} \times \cdots \times \\ &\begin{bmatrix} ie^{-ik_y} \sin(k_x - n\phi) & -e^{-ik_y} \cos(k_x - n\phi) \\ e^{ik_y} \cos(k_x - n\phi) & -ie^{ik_y} \sin(k_x - n\phi) \end{bmatrix} \begin{bmatrix} 1 \\ 0 \end{bmatrix} \end{aligned} \tag{S85}$$

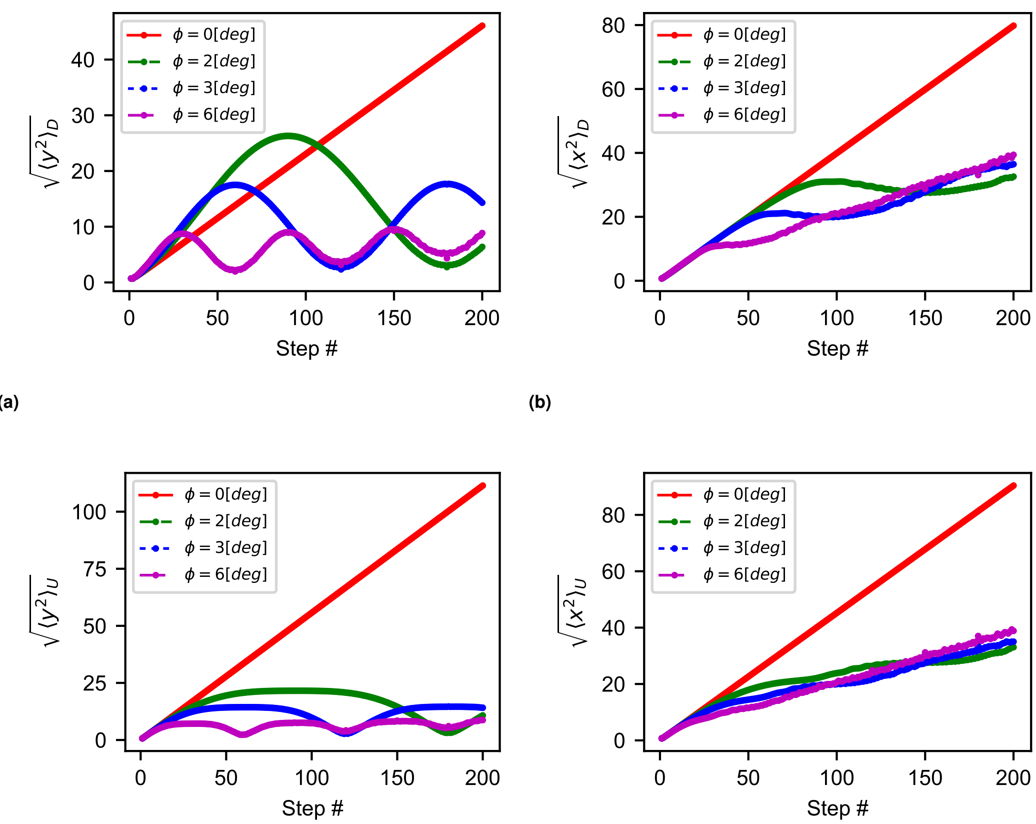

(c) (d)

Fig. S11. The quadratic mean of (a) y and (b) x for the down channel as a function of the time step for different phase modulation values. The quadratic mean of (c) y and (d) x for the up channel as a function of the time step for different phase modulation values.

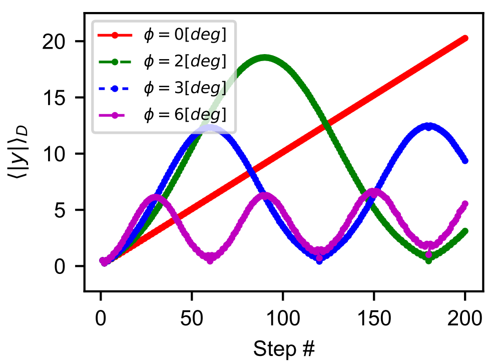

(a)

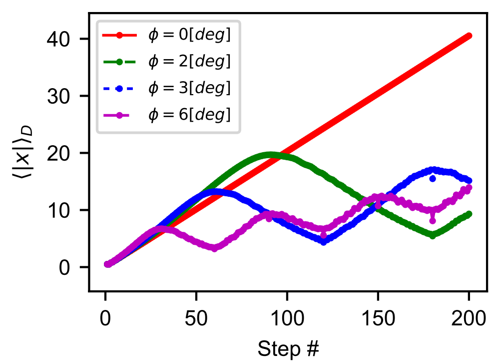

(b)

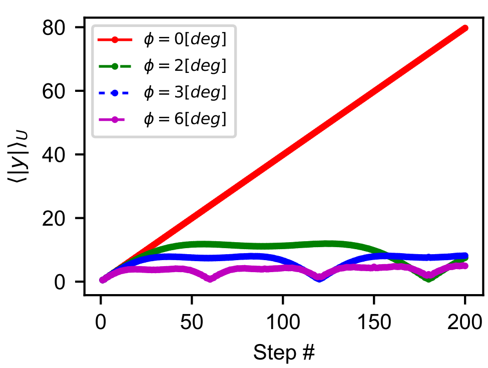

(c)

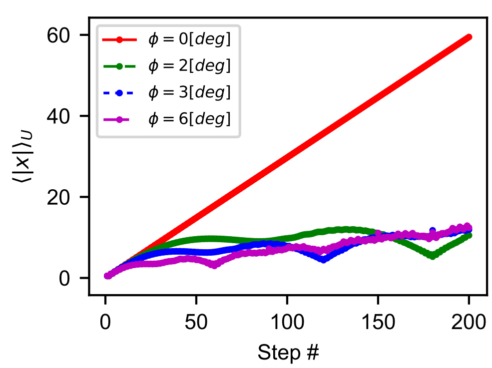

(d)

Fig. S12. The norm one of (a) y and (b) x for the down channel as a function of the time step for different phase modulation values. The norm one of (c) y and (d) x for the up channel as a function of the time step for different phase modulation values.

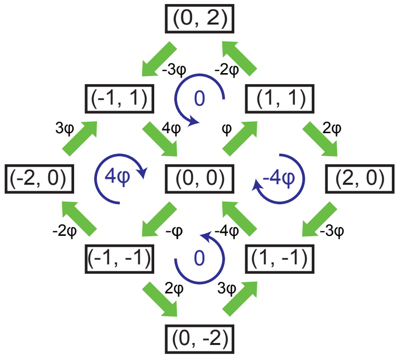

(a)

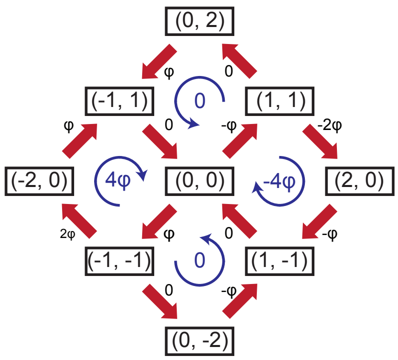

(b)

Fig. S13. (a) The accumulated phases based on time-varying gauge fields implemented in this work along four sample closed paths. (b) The accumulated phases using a coordinate-dependent unitary operation along four similar closed paths.

It is easy to verify that the expansion of $0.5\left(w^{(n)}_{k_x,k_y} - v^{(n)}_{k_x,k_y}\right)$ has terms proportional to $e^{ik_y n}$, $e^{ik_y(n-1)}$, ..., and $e^{ik_y(-n+2)}$. The first and last term represent the farthest y position from the x axis after n steps. By obtaining the amplitudes of these two terms based on the above equation, we can expand $0.5\left(w^{(n)}_{k_x,k_y} - v^{(n)}_{k_x,k_y}\right)$ as:

$$
\begin{aligned}
&0.5\left(w^{(n)}_{k_x,k_y} - v^{(n)}_{k_x,k_y}\right) \\
&= (-i)^{n-1}\, e^{ink_y} \cos\left(k_x - n\phi\right) \prod_{p=1}^{n-1} \sin\left(k_x - p\phi\right) \\
&+ i^{n-1} e^{-i(n-2)k_y} \cos\left(k_x - \phi\right) \prod_{p=2}^{n} \sin\left(k_x - p\phi\right) \\
&+ \sum_{y=-n+3}^{n-1} a_y\left(k_x, \phi, n\right) e^{ik_y y} \qquad \text{(S86)}
\end{aligned}
$$

Which means that

$$
\begin{aligned}
&P_D\left(y = -n\right) = P_D\left(y = n-2\right) \\
&= \frac{1}{2\pi} \int_{k_x=0}^{2\pi} \cos^2\left(k_x\right) \prod_{p=1}^{n-1} \sin^2\left(k_x - p\phi\right) dk_x. \qquad \text{(S87)}
\end{aligned}
$$

These expressions show the existence of zeros in the integrand at $k_x = p\phi$ for $p = 1$ to $n-1$. For $n \sim \frac{2\pi}{\phi}$, these zeros spread across the entire region of $k_x = 0$ to $k_x = 2\pi$. Especially, for the small values of ϕ, the presence of these zeros causes that $P_D\left(y = -n\right)$ and $P_D\left(y = n-2\right)$ tend to zero at $n \sim \frac{2\pi}{\phi}$. For other values of $y \neq 0$, similar expressions can be obtained for $P_D\left(y\right)$, which they also become small for $\phi = \frac{2\pi}{n}$. This analysis predicts that $\langle y^2\rangle_D$ tends toward zero for $n = 2\pi/\phi$.

Figures S11a and S11c summarize the numerical results for the variation of $\sqrt{\langle y^2\rangle_D}$ and $\sqrt{\langle y^2\rangle_U}$ with the time step for different values of ϕ. The obtained results show that for $1 \ll n \ll \pi/\phi$, $\sqrt{\langle y^2\rangle_D}$ varies as $n/\sqrt{6\pi}$, as one would expect from the zero phase modulation case. Moreover, the numerical results show that for small values of ϕ, $\sqrt{\langle y^2\rangle_D}$ reaches the maximum value at $n \cong \pi/\phi$. These results also show that $\langle y^2\rangle_D$ tends toward zero at $n \cong 2\pi/\phi$, which is consistent with the above analysis. The effect of phase modulation on the quadratic mean of x can be investigated as well. Numerical results as depicted in Figs. S11b and S11d show that the quadratic mean of x also decreases relative to the zero-phase modulation case. However, the effect of phase modulation is more intense on decreasing the quadratic mean of y as compared with the quadratic mean of x.

In addition to quadratic means, we can also look at the variations of the norm ones of the quantum walk distributions. Figures S12a and S12c summarize the numerical results for the variation of $\langle|y|\rangle_D$ and $\langle|y|\rangle_U$ with the time step for different values of ϕ. The corresponding results for the x direction are also shown in Figs. S12b and S12d.

B. Creation of electric fields using various gauge fields:

In addition to the time-dependent approach, an electric field can be implemented through the use of a coordinate-dependent gauge field as well. In the latter case, instead of using a time-dependent gauge field, a phase modulation is applied that is not direction dependent and instead depends on the coordinate linearly. In this approach, an effective linear electric potential $V = -\mathcal{E}x$ is implemented that will lead to the generation of an electric field based on $\overrightarrow{\mathcal{E}} = -\nabla V$. The unitary operation in each time step has an extra term relative to the standard quantum walk evolution operator U_0 as $U_\phi = e^{i\phi x}U_0$. We can compare the effect of such a gauge field with the time-dependent gauge field considered in this work. In Fig. S13, we have considered four sample closed paths that start from the origin and return to it, and have calculated the total phase accumulated in them. As this figure shows, the net amount of phase in both approaches are similar, showing that indeed the time-varying gauge field will induce a similar phase accumulation in these closed paths as a conventional electric field in the x direction. This similarity holds for any closed path starting from the origin and ending at it.

REFERENCES

1. H. Chalabi, S. Barik, S. Mittal, T. E. Murphy, M. Hafezi, and E. Waks, “Synthetic Gauge Field for Two-Dimensional Time-Multiplexed Quantum Random Walks,” Phys. Rev. Lett. **123**, 150503 (2019).